



## Application of 3-D Seismic Attributes Analysis for Structural Characterization and Hydrocarbon Prospectivity in “TLB” Field, Southern Niger Delta, Nigeria

Tasie B. Leslie, Thomas A. Harry, Ekefre E. Anyanime, Camillus Etim, Nsidibe Akata

Received: November 22, 2024 /Accepted: January 18, 2025

© REJOST 2025

### Abstract

This study investigates the hydrocarbon potential of the TLB Field, located in the southern Niger Delta, using well logs and 3D seismic data. The aim of this study is to evaluate the hydrocarbon potential of the TLB Field in the southern Niger Delta by utilizing 3D seismic attribute analysis and well log data for structural characterization and reservoir assessment. Through the integration of seismic attributes such as root mean square (RMS) amplitude, maximum magnitude, and variance, this study seeks to delineate hydrocarbon-bearing zones, identify key prospects, and estimate hydrocarbon volumes. These study gives precise understanding of the structural framework and reservoir quality within the field unlike previous studies. We analyzed seismic attributes such as root mean square (RMS) amplitude, maximum magnitude, and variance to delineate structural and stratigraphic features indicative of hydrocarbon-bearing zones. The structural interpretation of the seismic data revealed the presence of listric growth faults that play a significant role in hydrocarbon entrapment. Two reservoirs, Reservoir A (RES A) and Reservoir B (RES B), were identified at depths ranging from 3300 ft to 6400 ft. Reservoir A exhibited superior reservoir quality, with a porosity of 24% and a hydrocarbon saturation of 85%. Bright spot anomalies served as direct hydrocarbon indicators (DHIs), pointing to potential accumulation zones. The study identified three key prospects, designated as K, L, and M, with an estimated total of 20.6 million barrels of oil equivalent (MMBOE) and 199.1 million standard cubic feet (MSCF) of gas. The findings indicate that additional hydrocarbon leads exist within the field, suggesting that further exploration is warranted to maximize recovery.

---

✉ Thomas A. Harry: [tharry.tom@gmail.com](mailto:tharry.tom@gmail.com)

Department of Geology, Akwa Ibom State University

---

**Keywords:** Seismic Attributes, Hydrocarbon Prospectivity, Reservoir Characterization, Niger Delta Basin, RMS Amplitude, Fault Interpretation

## 1.0 Introduction

The Niger Delta Basin is one of the most prolific hydrocarbon provinces in the world, yet exploration remains a complex endeavor due to its intricate geological framework. This complexity arises from the interaction of tectonic forces and sedimentary processes, which have produced a heterogeneous subsurface with numerous faulted and stratigraphic traps (Doust & Omatsola, 1990). The TLB Field is located within the southern Niger Delta, an area characterized by extensive growth fault systems and deltaic sedimentation that has shaped the reservoir architecture.

Seismic attributes have become essential tools in hydrocarbon exploration, aiding in subsurface imaging and reservoir characterization. Since their introduction in the 1970s, these attributes have been widely applied to detect subtle changes in rock properties and fluid contacts, thereby improving the accuracy of hydrocarbon prediction. Taner (2001) highlighted the importance of attributes such as amplitude, phase, and frequency in detecting hydrocarbon accumulations. Recent studies by Akinloye *et al.* (2016) and Nwankwo *et al.* (2020) have further demonstrated the role of seismic attributes in fault mapping and stratigraphic interpretation within the Niger Delta. Advances in data processing techniques and machine learning applications have significantly improved the reliability of seismic inversion for hydrocarbon detection, as noted by Oluwole *et al.* (2022).

The geological framework of the Niger Delta Basin plays a critical role in hydrocarbon accumulation. The basin evolved through a series of tectonic events linked to the opening of the South Atlantic Ocean and the subsequent deposition of sediments from the Niger River system (Doust & Omatsola, 1990). It comprises three main formations: the Akata Formation, which serves as the primary source rock; the Agbada Formation, which consists of interbedded sands and shales that act as reservoir

units; and the Benin Formation, which forms the uppermost layer and provides regional sealing in some areas (Reijers *et al.*, 1996). The presence of growth faults, rollover anticlines, and other structural features enhances the hydrocarbon prospectivity of the basin. Dim (2016) emphasized the significance of structural traps in hydrocarbon accumulation, particularly in fault-dominated settings such as the Niger Delta.

Reservoir characterization in the Niger Delta relies on the assessment of key petrophysical properties, including porosity, net-to-gross ratio, water saturation, and hydrocarbon saturation. Studies by Ahmed (2010) and Dake (2001) indicate that high-porosity sands, typically greater than 20%, with water saturation values below 25%, are optimal for hydrocarbon storage and production. Similar hydrocarbon-bearing trends have been observed in the Uzot and Fuba fields, reinforcing the potential of the TLB Field as a productive hydrocarbon prospect (Ochoma *et al.*, 2023). In addition, direct hydrocarbon indicators (DHIs) such as bright spot anomalies on RMS amplitude maps have proven to be reliable markers of gas and oil accumulations. Bamidele *et al.* (2023) demonstrated the effectiveness of seismic attributes in identifying DHIs, particularly in regions where structural closures and stratigraphic traps play a key role in hydrocarbon retention.

Since their introduction in the 1970s, seismic attributes have become indispensable tools for subsurface imaging, aiding in the identification of hydrocarbon reservoirs (Taner, 2001). By quantifying seismic response characteristics such as amplitude, phase, and frequency, geoscientists can detect subtle changes in rock properties and fluid contacts (Avseth *et al.*, 2005). The application of 3D seismic attributes has proven to enhance the interpretation of complex subsurface features, making it possible to delineate hydrocarbon-bearing zones with greater accuracy (Bamidele *et al.*, 2023). In this study, seismic attribute analysis was applied to

characterize the structural framework of the TLB Field, map potential reservoirs, and evaluate hydrocarbon prospectivity.

## 2.0 Study Area and Geology

The TLB Field is located in the southern part of the Niger Delta Basin, which covers an area of approximately 70,000 km<sup>2</sup> (Whiteman, 1982). The basin extends along the Gulf of Guinea and is bounded by latitudes 3° to 6° N and longitudes 5° to 8° E. The Niger Delta was formed by the progradation of sediments supplied by the Niger, Benue, and Cross rivers and their distributaries. These sediments were deposited in a deltaic environment, leading to the formation of thick sequences of interbedded sands and shales (Adegoke *et al.*, 2017).

### 2.1 Basin Evolution and Tectonic Setting

The evolution of Niger Delta basin is related to the episodes of rifting and drifting apart of the African and South American plates which led to the opening of the South Atlantic Ocean (Reijers *et al.*, 1996). The rifting started and continued from late Jurassic till mid Cretaceous and the episode diminished in Late -Cretaceous (Lehner and De Ruiter, 1977). After the Atlantic Mesozoic rift, sedimentation started with deposits of Albian drift. The Benue Trough was filled with sediments and during Late Eocene, the basin started prograding into the current continental slope down to the deep sea. The continued pro-gradation of marine deposits since the Eocene extended to the current continental margin.

Cretaceous fracture zones occurring as trenches and ridges in the abyssal plains of the Atlantic Ocean controls the structural framework of the Niger delta (Dim, 2016). The ridges subdivide the continental margin of the South Atlantic Ocean into separate basins, forming the Cretaceous Benue-Abakaliki trough's border faults and cutting far into the shield of West Africa. The trough is a detached segment of a

triple rift intersection linked to the evolution of the South Atlantic Ocean.

The Niger Delta Basin comprises three primary stratigraphic units: the Akata, Agbada, and Benin Formations. The Akata Formation, composed mainly of marine shales, serves as the source rock for hydrocarbons. The overlying Agbada Formation contains interbedded sands and shales that form the primary reservoir units (Harry *et al.*, 2018). The Benin Formation, dominated by continental sands (Harry *et al.*, 2017), forms the uppermost layer and acts as a seal in some areas. Syn-depositional and post-depositional faulting has created numerous structural traps, enhancing the hydrocarbon potential of the region. Fig.1 and Fig. 2 below shows the Location and Base Map of TLB field respectively.

The TLB Field lies within a shallow offshore region characterized by growth faults, rollover anticlines, and horst-and-graben structures. These structural features play a critical role in hydrocarbon accumulation by forming traps that prevent the migration of hydrocarbons (Ibrahim *et al.*, 2023).

### 3.0 Methodology

This study utilized well logs and 3D seismic data to characterize the subsurface and identify hydrocarbon-bearing zones. The seismic data were processed using Schlumberger's Petrel software to generate various seismic attributes (Schlumberger, 2007). Well logs, including gamma-ray (GR), resistivity, and density logs, were used to correlate the reservoirs across multiple wells and validate the seismic interpretation (Akinloye *et al.*, 2016). The seismic interpretation involved mapping faults and horizons to understand the structural framework of the TLB Field. Time surfaces were generated and converted to depth using a second-order polynomial velocity model to ensure accurate spatial representation of geological features.

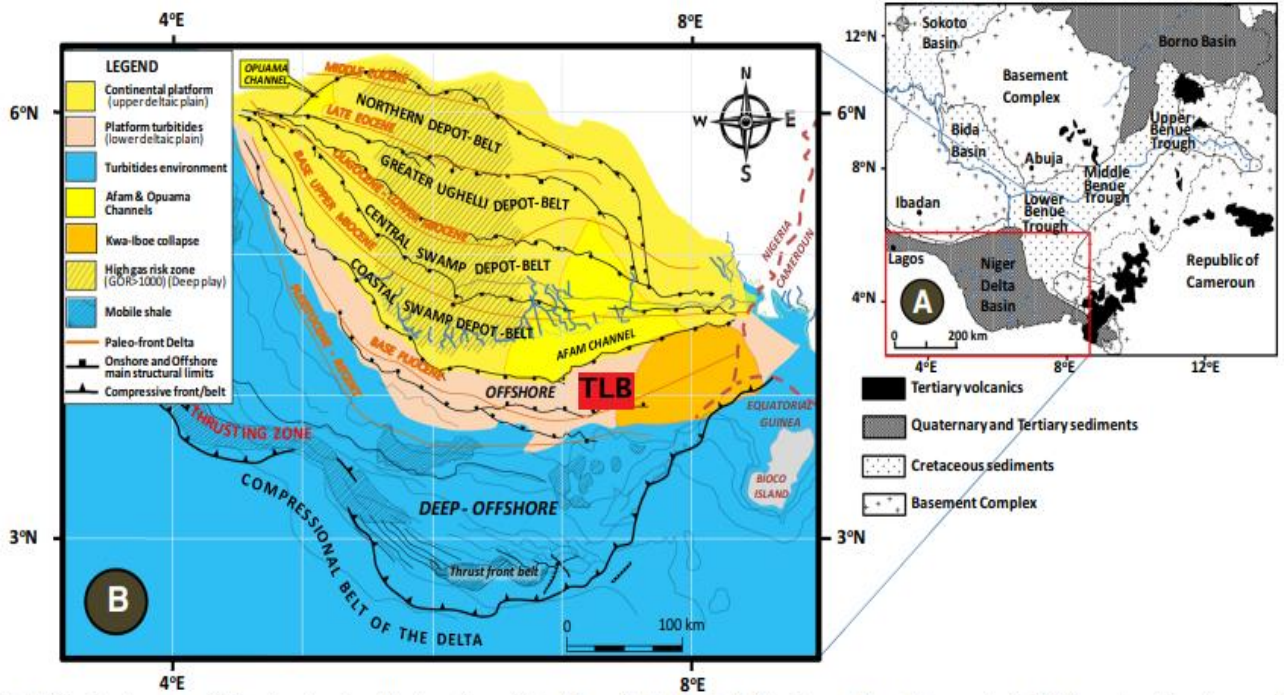


Fig.1: Geologic map of Nigeria showing the location of the Niger Delta Basin (a) (redrawn from Ebong et al, 2017) and sectional map of Niger Delta depositselts showing the studied field TLB.(b) (Redrawn from Doust and Omatsola, 1990).

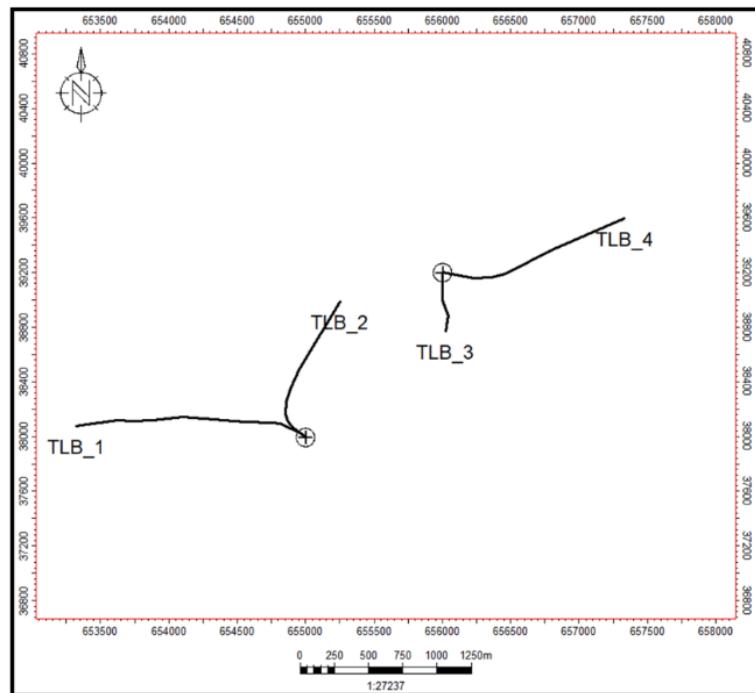


Fig.2: Base Map of the study Area.

Seismic attributes such as RMS amplitude, maximum amplitude, and variance were extracted to highlight potential hydrocarbon zones. RMS amplitude maps were used to detect bright spot anomalies (associated with hydrocarbons, while variance attributes helped delineate faults and stratigraphic discontinuities

(Ajisafe & Ako, 2013). The petrophysical analysis focused on evaluating key reservoir properties, including porosity, net-to-gross (N/G) ratio, and hydrocarbon saturation ( $S_h$ ). These parameters were computed for each reservoir to assess their capacity for hydrocarbon storage and production (Harry and

Akata, 2019). Volumetric estimation of the original hydrocarbon in place makes use of static parameters such as the area of accumulation (A), pay thickness ( $h$ ), porosity ( $\phi$ ), and initial fluids saturation ( $S_w$ ) of the reservoir. The estimation of hydrocarbon at reservoir condition (HIIP) can be done using:

$$HIIP = A \times h \times \phi \times (1 - S_w) \quad (1)$$

described in Ahmed (2010) and Craft & Hawkins (1991).

The percentage of the void space within the reservoir is calculated as the product of the GRV and porosity ( $\phi$ ), the value of the original oil-in-place (OOIP), expressed in reservoir barrels (RB) and can be estimated when the void space containing oil is multiplied by oil saturation ( $S_h$ ) and formation volume factors (FVF) are applied to convert the resultant volumes. The OOIP is expressed in stock tank barrels (STB) and can also be expressed in reservoir barrels (RB) by making use of the oil formation volume factor (FVF).

$$HIIP = \frac{GRV \times NTG \times \phi \times S_h}{FVF} \quad (2)$$

The hydrocarbon resource evaluation was carried out using the basic volumetric formulas.

The value of the Stock-tank-oil-in-place (STOIP) is given by (Dake, L. P. (2001):

$$STOIP = 7758 \frac{GRV \times NTG \times \phi \times S_o}{B_o} \quad (3)$$

where STOIP = stock tank oil-in-place (STB),

GRV = Gross Rock Volume (acre-ft.), NTG = Net to Gross ratio,  $\phi$  = porosity,  $S_o$  = Oil Saturation ( $1 - S_w$ ),  $B_o$  = Oil formation factor (RB/STB), (Expansion factor =  $1/B_o$  which is a "shrinkage factor" as  $B_o > 1$ ) (Economides *et al.*, 1994)

Gas-initially-in-place (GIIP) was calculated using:

$$GIIP = 43560 \frac{GRV \times NTG \times \phi \times S_g}{B_g} \quad (4)$$

where GIIP = gas-initially-in-place ( $\text{ft}^3$ ), GRV = gross rock volume (acre-ft.), NTG = net/gross ratio,  $S_g$  = gas saturation (fraction),  $B_g$  = gas formation factor (RCF/SCF) (Expansion factor =  $1/B_g$  as  $B_g < 1$ ).

#### 4.0 Results and Interpretation

The correlation of well data revealed two primary reservoirs, designated as RES A and RES B. These reservoirs were identified within the Agbada Formation and displayed distinct petrophysical characteristics.

The RES A was encountered at depths ranging from 3300 to 6000 ft across four wells. The petrophysical analysis indicated that RES A had an average porosity of 24%, a net-to-gross ratio of 74%, and a hydrocarbon saturation of 85%. The net pay thickness varied across the wells, with TLB-1 showing an oil pay thickness of 69 ft and TLB-3 exhibiting a gas pay thickness of 28 ft. The high porosity and hydrocarbon saturation suggest that Reservoir A is an excellent candidate for hydrocarbon production. Fig.3 above shows the display of B to B<sup>1</sup> correlation of hydrocarbon bearing sands across wells in the 'TLB' field; the large resistivity spikes indicate the presence of Hydrocarbon.

The RES B was encountered at greater depths, ranging from 3600 to 6400 ft. This reservoir displayed an average porosity of 23% and a net-to-gross ratio of 76%, with water saturation averaging 21% (Ojo *et al.*, 2018). The reservoir was well-connected across the wells, with oil and gas pay thicknesses varying between 22 ft and 81 ft.

The seismic interpretation revealed the presence of listric normal growth faults that formed horst-and-graben structures. Thirty-five faults were mapped, including synthetic and antithetic faults that contributed to the formation of structural traps. The fault systems were oriented in a northwest-southeast direction and provided the structural closures necessary for hydrocarbon entrapment.

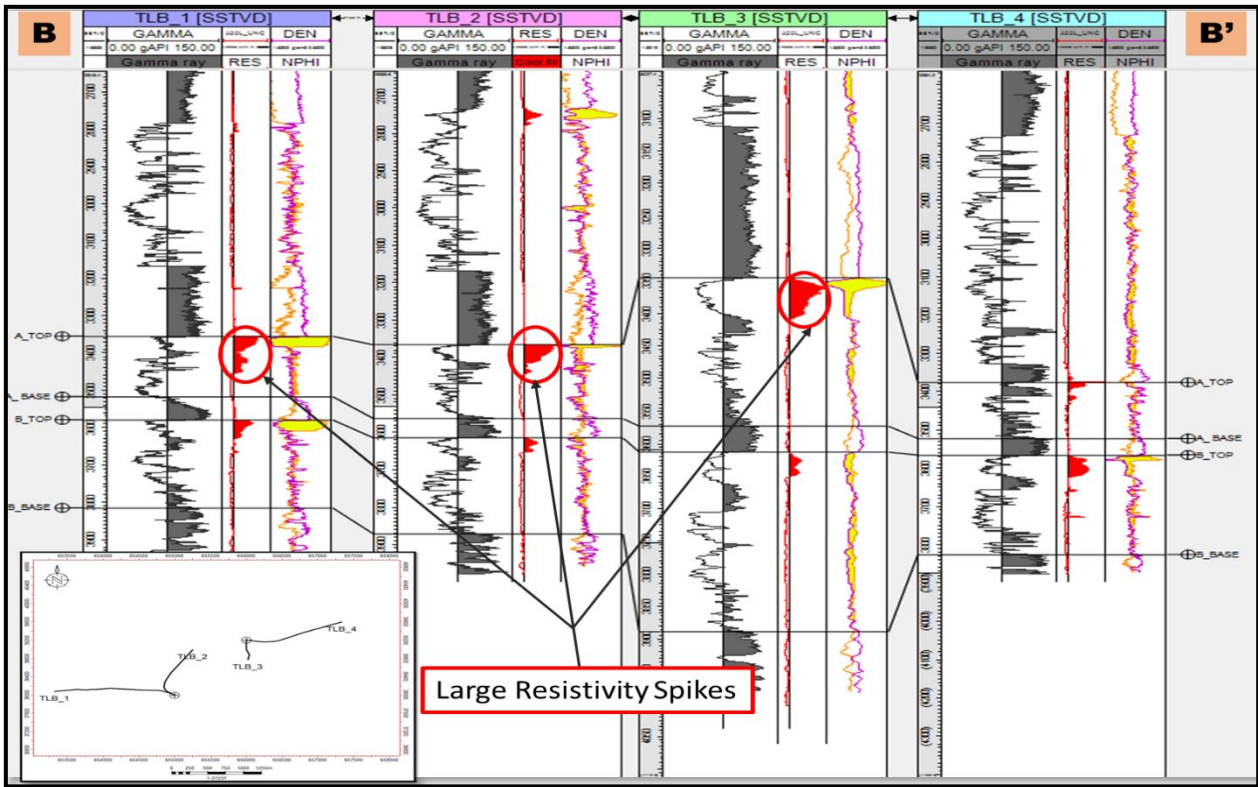


Fig. 3: Display of B to B’ correlation of hydrocarbon bearing sand across wells in the “TLB” field. (Large resistivity spikes indicates presence of hydrocarbon)

The RMS amplitude maps highlighted bright spot anomalies in both reservoirs, indicating the presence of hydrocarbons. In RES A, the RMS amplitude values ranged from 0 to 36,000, while RES B exhibited values up to 54,000.

These anomalies were concentrated in regions with high porosity sands, confirming the presence of hydrocarbon-filled reservoirs

Fig. 4 and 5 shows the Petrophysical summaries for RES A and RES B respectively, While Fig.6 and 7 shows the plot of net pay thickness for Reservoir A and B respectively. Variance attribute maps further revealed major discontinuities, enhancing the identification of fault zones and stratigraphic features (Law & Chung, 2006).

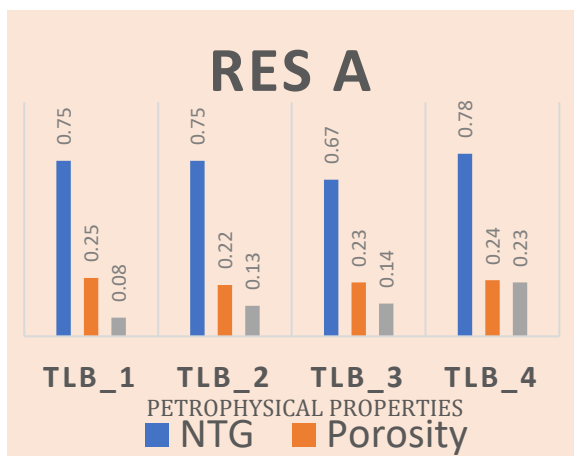


Fig. 4: Petrophysical summary plot for the Res A interval.



Fig. 5: Petrophysical summary plot for the RES B interval

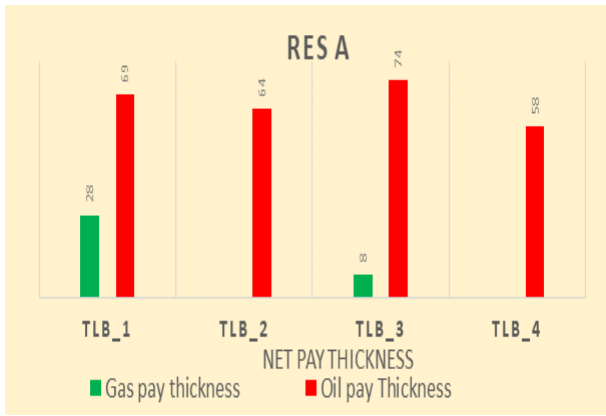


Fig. 6. Plot of net pay thickness for Res A

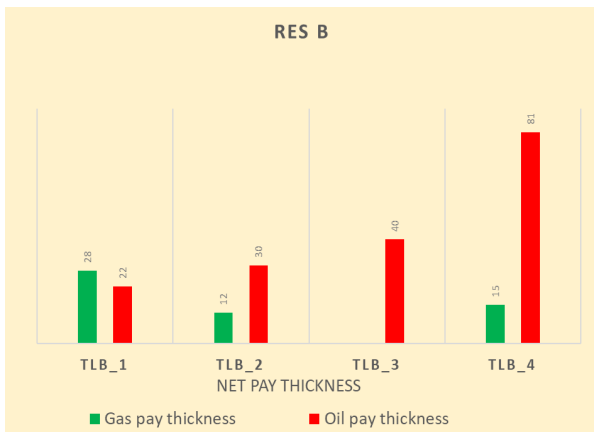


Fig. 7. Plot of net pay thickness for Res A

### 4.1 Prospect Identification and Volumetric Estimation

The analysis identified three key hydrocarbon prospects within Reservoir A, designated as Prospects K, L, and M. These prospects were characterized by high RMS amplitude values and were associated with fault-bounded closures (Obi *et al.*, 2021).

Time Contour maps showing the most accurate representative geology of reservoir A and B is presented in Fig. 8a. The maps show the major faults that formed the closure that contributes to the accumulation of hydrocarbon in the Field.

### 4.2 Depth Surface

The resultant depth residual values generated using the 2nd order polynomials velocity model (Figure 8b) was used for converting A and B reservoirs from time to depth because it has the least residuals. The depth converted reservoir A and B surfaces are presented in Fig.9, for the second order polynomial velocity function.

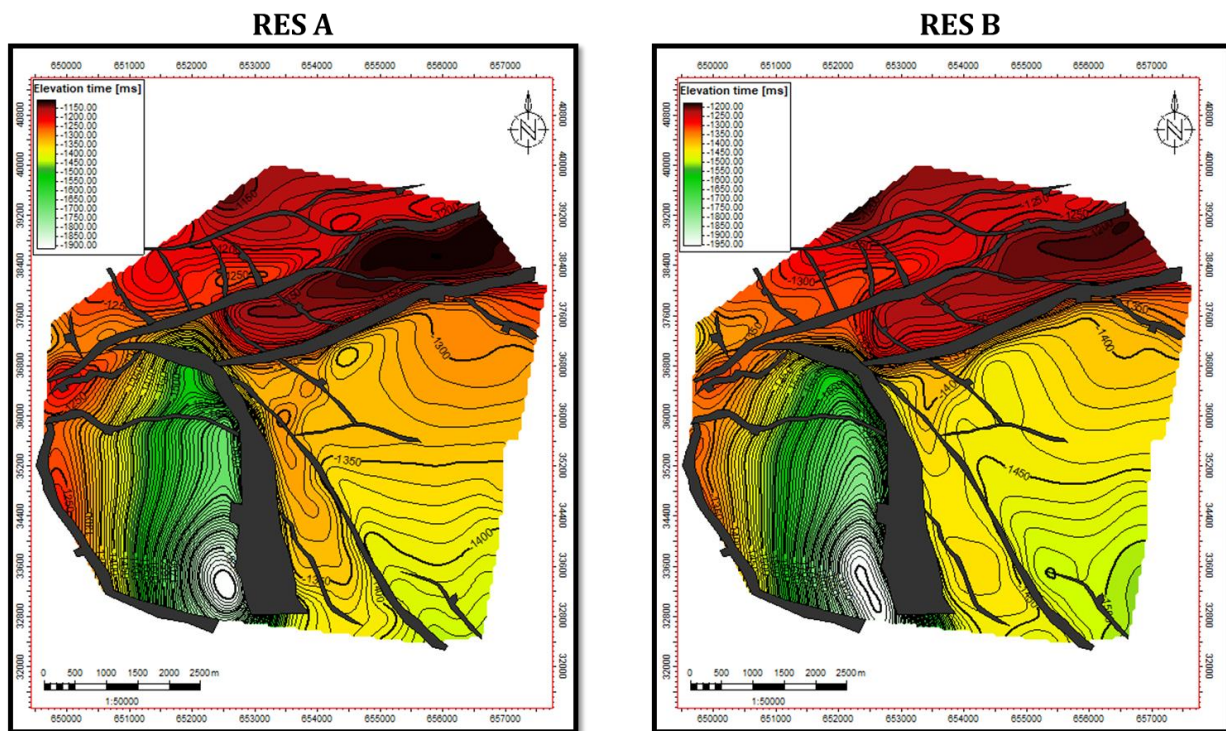


Fig. 8a: Time Maps for reservoir A and B showing the fault structures of the field.

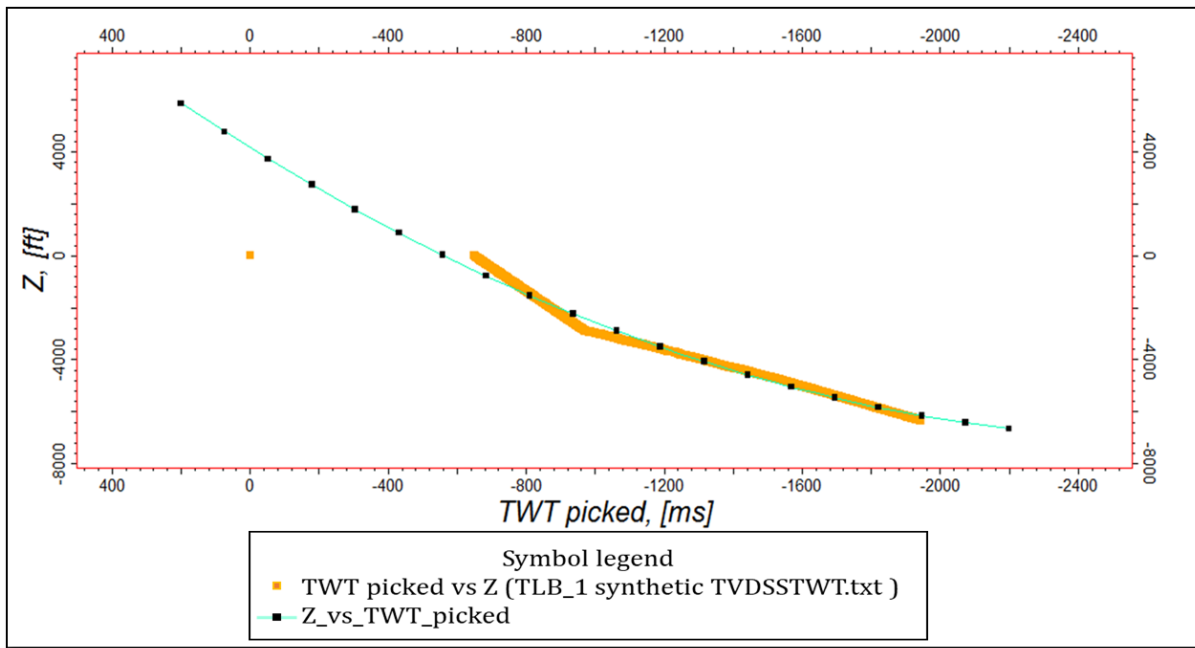


Fig.8b: Velocity model showing the time to depth relationship

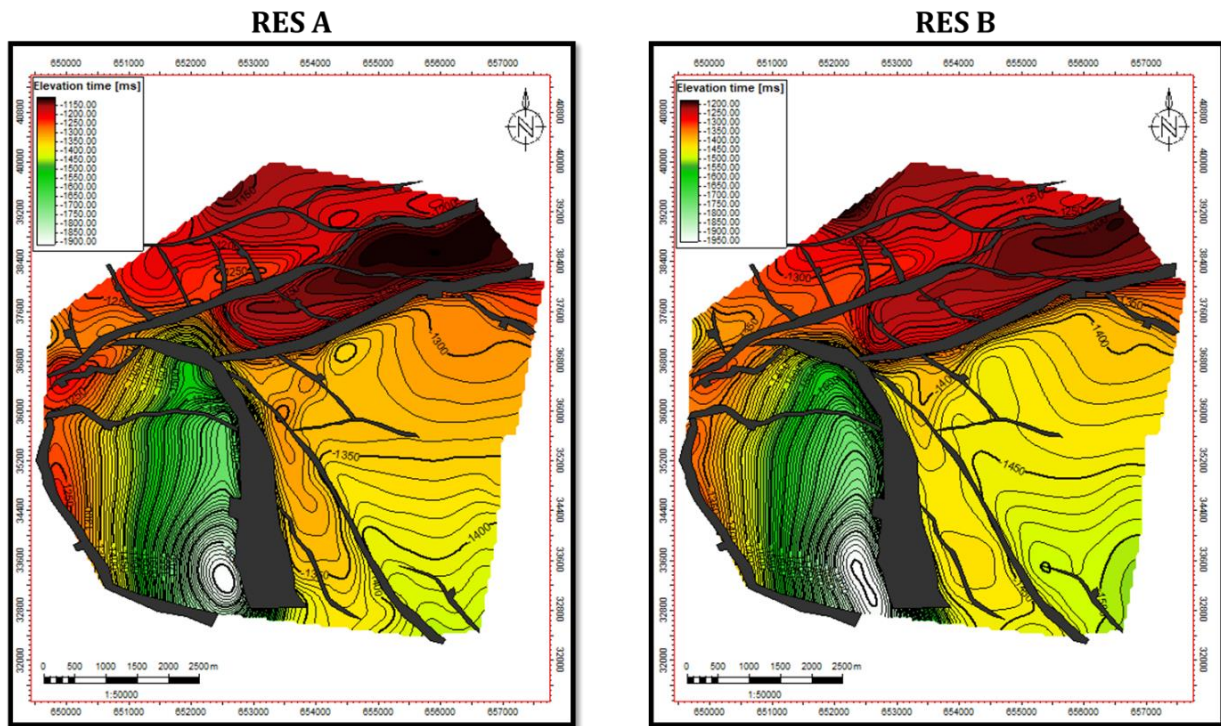
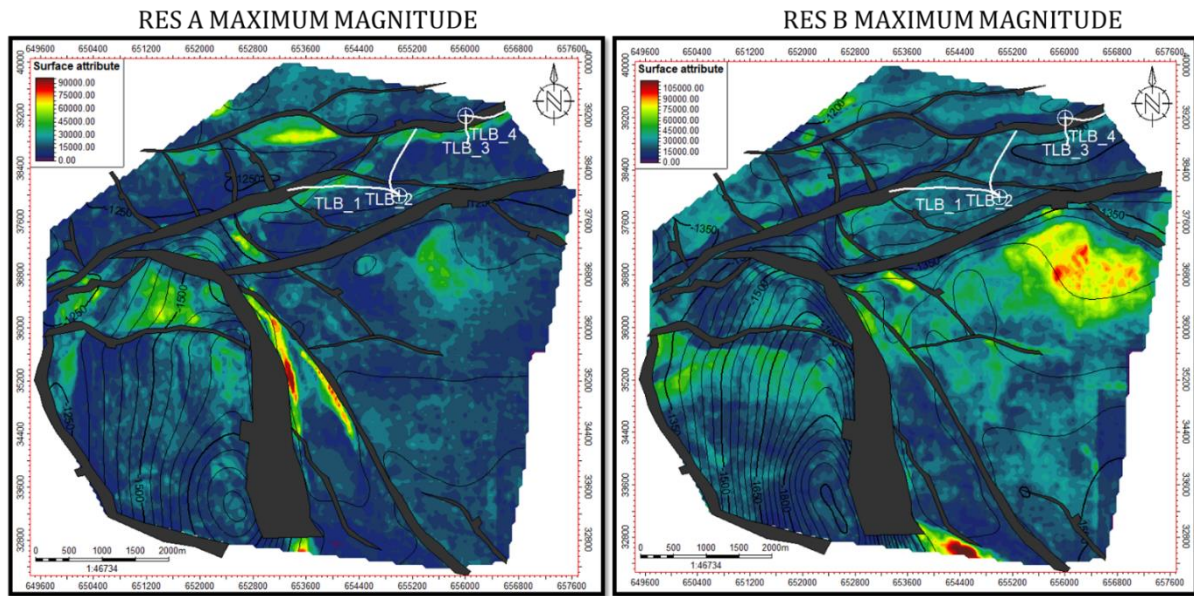


Fig 9: Depth Maps for reservoir A and B showing the fault structures of the field

**4.3 Time Surface**

The depth structure maps reveal that the reservoirs are anticlinal and fault supported. Reservoir A is found at a shallower depth from 3300 to 6000 ft while reservoir B is found at a deeper depth ranging from 3600 to 6400ft respectively. The RMS amplitude maps, maximum amplitude maps, maximum magnitude maps and average magnitude maps

generated for all the studied surfaces (Reservoir A and B) showed that strong amplitude anomalies exist at the Northern and North Western part of the field in RES A while the Eastern parts of the field exhibit high Amplitudes in RES B; seen as bright spots in the Fig.10, Fig. 11 and Fig. 12 from the generated maximum magnitude maps from the surfaces of RES A and REV B.



**Fig.10:** Generated Maximum Magnitude Maps for Reservoir Surface A and B

The parts of the field where these strong amplitude anomalies were observed corresponds to the observed anticlinal structure in the field. Other parts of the field where the amplitude anomalies were observed also correspond to the identified structural closures found in the field. Results indicate that strong amplitude anomalies are structurally controlled as they are seen occurring near faults on structural maps. The RMS amplitude maps, maximum amplitude maps, maximum magnitude maps and average magnitude maps

generated for all the studied surfaces presented were seen to have similar patterns of bright spot anomaly, which are likely associated with of facies and/or fluid content. In addition, these anomalies are seen on structural high, which suggested prospect conformity with regional structural high. The RMS amplitude values range from 0 (purple) to 36,000 (red) in reservoir A and from 0 (purple) to 54,000 (red) in reservoir B. The red-yellowish color represents hydrocarbon sands.

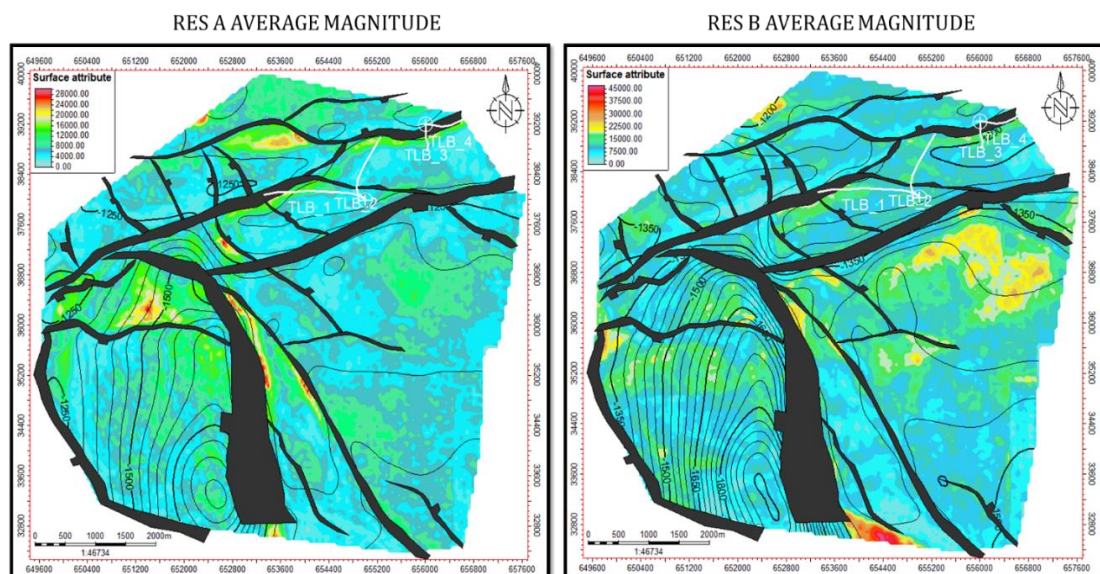


**Fig. 11:** Generated Average Magnitude Maps for Reservoir Surface A and B

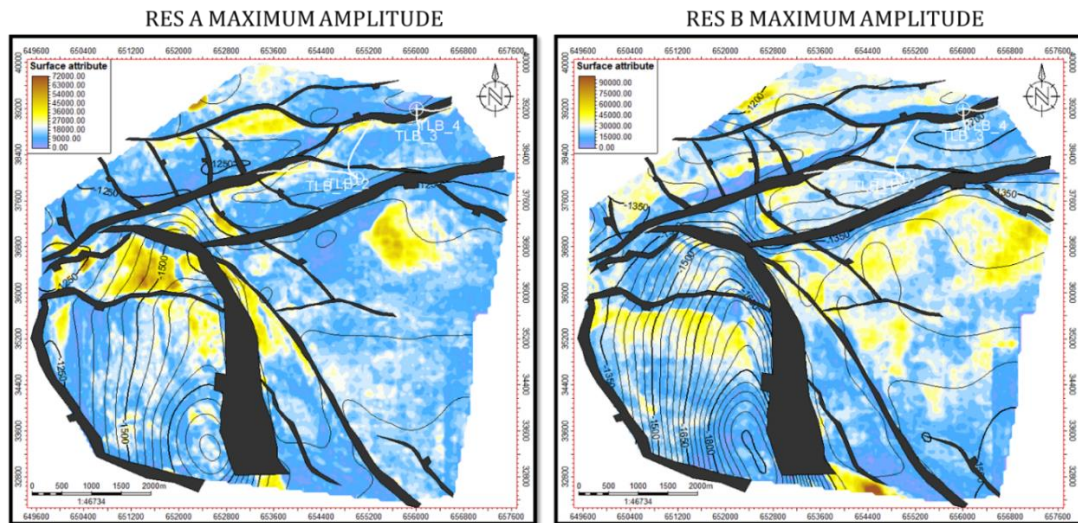


Fig. 12: Generated Maximum Amplitude Maps for Reservoir Surface A and B

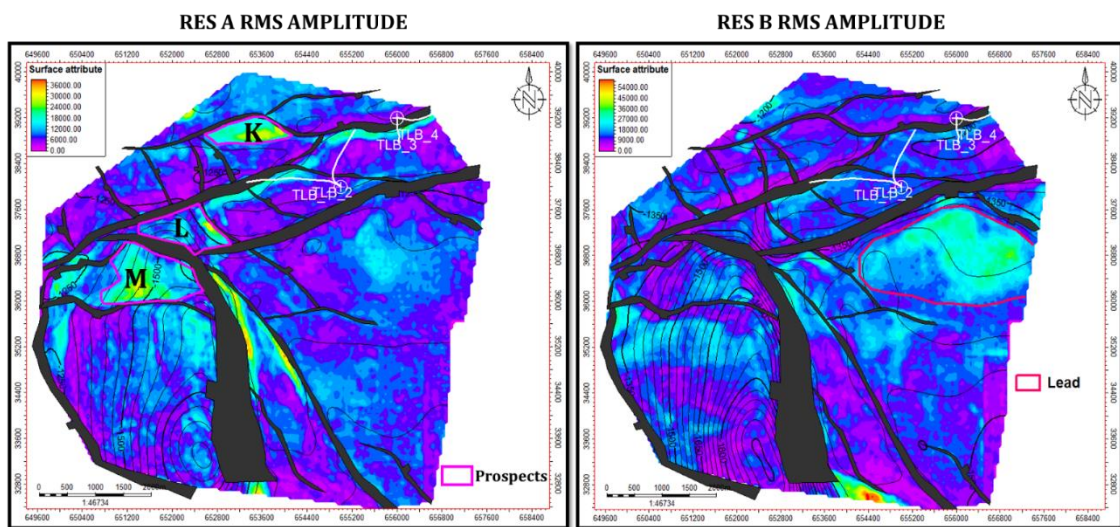


Fig. 13: Identified Fault-block based prospects using the RMS amplitude for RES A and REV B

#### 4.4 Evaluation of Identified Prospects

Seismic attributes analysis carried out within the study area revealed prospective zones where the drilled wells did not penetrate. RMS amplitude attributes was selected and used in this study because of its application as Direct Hydrocarbon Indicators (HDI) (Fig. 13). Correlating these attributes with the structural closures as seen on the depth structure maps depicts the presence of prospective zones within these areas. Three prospects (prospect K, prospect L, and prospect M) were identified based on the seismic attributes interpreted on time slices and vertical transects. The anomalies were identified based on their response to the seismic attributes,

which are indicative of the presence of hydrocarbon accumulations. High values of original amplitudes (Fig. 13) and localized high values of RMS amplitude attribute within the high original amplitude region reinforce the interpretation of hydrocarbon-filled sand. Fig.13 shows the Identified Fault-block based prospects using the RMS amplitude for RES A and REV B. Prospect K was located in the northwestern part of the field and exhibited strong amplitude anomalies consistent with oil-bearing sands. Prospect L, situated near the central portion of the field, was identified as a fault-bounded anticline with an estimated stock tank oil initially in place (STOIP) of 8.2 million barrels

of oil equivalent (Ajisafe & Ako, 2013). Prospect M was located in the eastern part of the field and exhibited gas potential, with a gas initially in place (GIIP) estimate of 77.8 million

standard cubic feet. Table 1 below shows the derived parameters used for the volumetric calculations for Prospects K, L and M respectively.

**Table 1:** Parameters and results of Volumetric calculation for identified prospects of 'TLB' Field

PROSPECT	Area (acre)	GRV (acre.ft)	N/G	PHI	Sw	Boi	Bgi	STOIIP (MMBOE)	GIIP (MCF)
Prospect K	105.48	5978.05	0.74	0.24	0.15	1.25	0.8	3.7	49.2
Prospect L	116.238	8762.34	0.74	0.24	0.15	1.25	0.8	8.2	72.1
Prospect M	134.48	9460.97	0.74	0.24	0.15	1.25	0.8	8.7	77.8

## 5.0 Discussion

The structural interpretation and attribute analysis of the TLB Field confirmed the presence of significant hydrocarbon reserves. Bright spot anomalies identified in the RMS amplitude maps corresponded to zones of high fluid saturation, reinforcing the reliability of seismic attributes as direct hydrocarbon indicators. The identification of fault-controlled structural closures further suggests that hydrocarbons are effectively trapped within the reservoirs.

The analysis conducted in this study identified three key hydrocarbon prospects within the TLB Field, designated as Prospects K, L, and M. These prospects were found within two main reservoirs, Reservoir A and Reservoir B. Reservoir A, encountered at depths ranging from 3300 to 6000 feet, exhibited a porosity of 24%, a net-to-gross ratio of 74%, and a hydrocarbon saturation of 85%. Reservoir B, found at depths between 3600 and 6400 feet, had slightly lower porosity at 23% but maintained a high net-to-gross ratio of 76% with a hydrocarbon saturation of 79%. The petrophysical evaluation confirmed that both reservoirs possess favorable conditions for hydrocarbon accumulation, with significant

hydrocarbon columns and well-connected reservoir systems.

Prospect K, located in the northwestern part of the field, exhibited strong amplitude anomalies indicative of oil-bearing sands, with an estimated hydrocarbon volume of 3.7 million barrels of oil equivalent (MMBOE) and 49.2 million standard cubic feet (MSCF) of gas. Prospect L, situated near the central portion of the field, was identified as a fault-bounded anticline with an estimated stock tank oil initially in place (STOIIP) of 8.2 MMBOE and 72.1 MSCF of gas. Prospect M, located in the eastern part of the field, was primarily a gas prospect, with a gas initially in place (GIIP) estimate of 77.8 MSCF and an oil estimate of 8.7 MMBOE. The seismic interpretation revealed that these prospects were structurally controlled, with high RMS amplitude values corresponding to hydrocarbon-filled sands.

The study further confirmed that fault-controlled closures play a crucial role in hydrocarbon entrapment in the TLB Field. A total of 35 faults were mapped, including listric growth faults that contributed to the formation of horst-and-graben structures. Depth maps of the field showed that the reservoirs are anticlinal and fault-supported,

further enhancing their ability to trap hydrocarbons. RMS amplitude maps, maximum amplitude maps, and variance attributes consistently highlighted bright spot anomalies that correspond to hydrocarbon-bearing zones. Law & Chung (2006) emphasized the use of variance attributes in delineating stratigraphic discontinuities, which is particularly relevant in identifying reservoir heterogeneity and fault compartmentalization.

The integration of structural interpretation, seismic attribute analysis, and petrophysical evaluation supports the conclusion that the TLB Field contains commercially viable hydrocarbon reserves. The bright spot anomalies identified in the RMS amplitude maps correlate strongly with zones of high fluid saturation, reinforcing the reliability of seismic attributes as DHIs. Comparative analysis with other fields in the Niger Delta suggests that the TLB Field shares similar structural styles and amplitude responses with established hydrocarbon-bearing trends. The presence of favorable reservoir properties, including high porosity, low water saturation, and strong net-to-gross ratios, coupled with well-defined trapping mechanisms, confirms the prospectivity of the field.

## **6.0 Summary and Conclusion**

The detailed evaluation of the TLB Field, integrating structural interpretation, seismic attribute analysis, and petrophysical characterization, has confirmed the presence of significant hydrocarbon reserves within Reservoirs A and B. The RMS amplitude anomalies correspond to zones of high fluid saturation, validating the seismic interpretation as a reliable direct hydrocarbon indicator. The fault-controlled structural closures provide robust trapping mechanisms, ensuring hydrocarbon retention within the reservoirs.

Reservoir A was encountered at consistent depths across the wells, indicating lateral continuity and minimal structural heterogeneity.

With a gross thickness of 1377 ft, an average net-to-gross (N/G) ratio of 0.74, porosity of 0.24, and low water saturation of 0.15, the reservoir demonstrates favorable conditions for hydrocarbon accumulation and production. These petrophysical properties suggest that Reservoir A has a strong production potential, particularly given its extensive hydrocarbon column and well-connected reservoir system.

Reservoir B, encountered at varying depths across the wells, displayed some structural variability but maintained overall continuity. The reservoir's gross thickness of 1918 ft and an N/G ratio of 0.76 indicate a substantial hydrocarbon-bearing interval. The average porosity of 0.23 and water saturation of 0.21 further support the classification of Reservoir B as a high-quality reservoir. The net pay thickness analysis revealed variable gas and oil distributions, with notable oil pay zones in wells TLB\_3 and TLB\_4, suggesting localized zones of enhanced reservoir quality, likely influenced by structural highs or hydrocarbon migration pathways.

The distribution of hydrocarbon-bearing intervals across the TLB Field highlights the importance of detailed reservoir characterization to identify optimal production zones and understand reservoir compartmentalization. Despite some variability in fluid distribution, the petrophysical properties across both reservoirs consistently indicate favorable reservoir conditions for hydrocarbon recovery.

In conclusion, the integration of seismic attribute analysis, structural interpretation, and petrophysical data has demonstrated that the TLB Field is a commercially viable prospect. The presence of fault-controlled closures, combined with favorable reservoir properties, supports significant hydrocarbon accumulation and retention within the field. Both Reservoirs A and B exhibit strong production potential, with Reservoir B demonstrating particularly high oil

pay intervals in some wells. These findings indicate that the TLB Field represents a promising target for hydrocarbon development and production, warranting further appraisal and development planning to optimize recovery strategies.

## References

- Adeyayo, S., Ijeoma, T., Folake, M., & Daniel, O. (2022). Assessing reservoir quality and fluid distribution using seismic attributes in the Niger Delta. *Energy Exploration & Exploitation*, 40(4), 897–912.
- Adegoke, O. S., Oyebamiji, A. S., Edet, J. J., Osterloff, P. L., & Ulu, O. K. (2017). *Cenozoic Foraminifera and Calcareous Nannofossil Biostratigraphy of the Niger Delta*. Elsevier.
- Ahmed, T. (2010). *Reservoir engineering handbook* (4th ed.). Gulf Professional Publishing.
- Akinloye, O., Olugbenga, O., Adebayo, S., & Chika, A. (2016). Application of seismic attributes for fault analysis in the Niger Delta. *Journal of Geophysics and Engineering*, 13(4), 852–867.
- Ajisafe, O., & Ako, B. (2013). The application of seismic attributes in hydrocarbon reservoir characterization: A case study from the Niger Delta. *Geophysics Journal International*, 195(2), 354–368.
- Avseth, P., Mukerji, T., & Mavko, G. (2005). *Quantitative seismic interpretation*. Cambridge University Press.
- Bamidele, T., Samuel, O., Chika, S., & Oluwaseun, F. (2023). Challenges in seismic attribute analysis for the Niger Delta: Insights and solutions. *Geophysical Journal International*, 232(3), 1176–1190.
- Craft, B. C., & Hawkins, M. F. (1991). *Applied petroleum reservoir engineering* (2nd ed.). Prentice Hall.
- Dake, L. P. (2001). *Fundamentals of reservoir engineering*. Elsevier.
- Dim, C. I. (2016). Evolution and petroleum systems of the Niger Delta Basin, Nigeria. *Journal of Petroleum Exploration and Production Technology*, 6(2), 371–382.
- Doust, H., & Omatsola, E. (1990). Niger Delta. In J. D. Edwards & P. A. Santogrossi (Eds.), *Divergent/passive margin basins* (Vol. 48, pp. 239–248). AAPG Memoir.
- Economides, M. J., Hill, A. D., & Ehlig-Economides, C. (1994). *Petroleum production systems*. Prentice Hall.
- Ebong, E. D., Akpan, A. E., Emeka, C. N., & Urang, J. G. (2017). Groundwater quality assessment using geoelectrical and geochemical approaches: Case study of Abi Area, southeastern Nigeria. *Journal of Applied Water Science*, 7(5), 2463–2478.
- Harry, T. A., Bassey, C. E., Udofia, P. A., & Daniel, S. (2017). Baseline study of estuarine oceanographic effects on benthic foraminifera in Qua Iboe, Eastern Obolo, and Uta Ewa/Opobo River Estuaries, Southeastern Nigeria. *International Journal of Scientific and Engineering Research*, 8(7), 1422–1331.
- Harry, T. A., Etuk, S. E., Joseph, I. N., & Austin, O. E. (2018). Geomechanical evaluation of reservoirs in the coastal swamp, Niger Delta Region, Nigeria. *International Journal of Advanced Geosciences*, 6(2), 165–172.
- Harry, T. A., & Akata, N. I. (2019). Evaluation of shale volume and effective porosity from wireline logs in “Watty” Field, Niger Delta, Nigeria. *International Journal of Scientific*

- & *Engineering Research*, 10(12), 1150–1158.
- Ibrahim, S., Esther, O., Chuka, K., & Solomon, D. (2023). Integration of seismic attributes with remote sensing data for enhanced exploration in the Niger Delta. *Computers & Geosciences*, 133, 105616.
- Law, W. K., & Chung, A. S. C. (2006). Minimal weighted local variance as edge detector for active contour models. In P. J. Narayanan (Ed.), *Lecture Notes in Computer Science* (pp. 622–632).
- Lehner, P., & De Ruiter, P. A. C. (1977). Structural history of the Atlantic margin of Africa. *AAPG Bulletin*, 61(7), 961–981.
- Nwankwo, E., Ijeoma, C., Daniel, A., & Bamidele, S. (2020). Evaluation of hydrocarbon prospectivity using seismic attributes in the Niger Delta. *Energy Exploration & Exploitation*, 38(6), 2112–2130.
- Ojo, J., Adewale, T., Emmanuel, S., & Folake, K. (2018). Using seismic attributes to characterize faults and fractures in the Niger Delta Basin. *Geophysical Prospecting*, 66(1), 123–138.
- Ochoma, S., Chinedu, A., & Uche, O. (2023). Comparative analysis of hydrocarbon-bearing trends in the Niger Delta: A case study of the Uzot and Fuba fields. *Petroleum Geoscience*, 29(1), 47–63.
- Obi, C. A., Nwosu, J. I., & Ezech, E. (2021). Structural interpretation and reservoir characterization using seismic attributes in the Niger Delta. *Journal of Petroleum Geoscience and Engineering*, 40(2), 102–115.
- Oluwole, J., Bukola, A., Emmanuel, N., & Kemi, A. (2022). Application of advanced seismic attributes and data processing techniques in the Niger Delta. *Journal of Applied Geophysics*, 192, 104321.
- Reijers, T. J. A., Petters, S. W., & Nwajide, C. S. (1996). The Niger Delta Basin. In T. J. A. Reijers (Ed.), *Selected chapters on geology: Sedimentary geology and sequence stratigraphy of the Niger Delta* (pp. 103–122). SPDC Corporate Reprographic Services.
- Schlumberger. (2007). *Interpreter's guide to seismic attributes*. Schlumberger Ltd.
- Taner, M. T. (2001). Seismic attributes. *Canadian Society of Exploration Geophysicists Recorder*, 26(9), 48–56.
- Whiteman, A. (1982). *Nigeria: Its petroleum ecology, resources, and potential*. Graham and Trotman.